Crystal and molecular structures of alkali oxalates – first proof of a staggered oxalate anion in the solid state

R.E. Dinnebier, S. Vensky, and M. Jansen

Alkali oxalates play an important role in nature and chemistry. The sodium and potassium salts of oxalic acid are found in many plants (clover, sorrel, salicornia, spinach, rhubarb, bamboo shoots, cacao, roots, and tree barks). Oxalates find some technical and medical applications such as stain removal in photography, metal coatings for stainless steel, nickel, chromium, titanium and their alloys, cleaning and bleaching of natural fibers, textile dyeing, anticoagulants in medical tests, and dental seals. Furthermore potassium and sodium oxalate complexes are able to pass the gastric mucous membrane and therefore they are the main components of kidney stones.

Nevertheless, the long-standing efforts aimed at understanding the characteristic structural features of the oxalate anion using conventional concepts of chemical bonding still remain without a closure. In the first place, the C–C bond lengths of oxalates anions (1.567(2) Å) are about 0.04 Å too large for two sp^2 hybridized C atoms (1.515 Å). This well-established experimental fact is indicative for a bond order of one or even less.

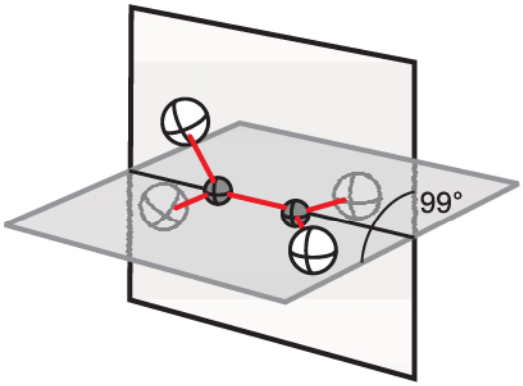

Figure 11: Sketch of the oxalate anion as found in $Cs_2C_2O_4$.

Thus, one would expect a staggered conformation (point symmetry D_{2d}) of the oxalate anions to be preferred (Fig. 11). This view is strongly supported by quantum mechanical calculations. However, experimentally the opposite is found: only few exceptions from planarity (D_{2h}) have been reported so far. If crystal structures with R-values >14% are disregarded, only $NaHC_2O_4 \cdot H_2O$ (twist angle of 13°), KHC_2O_4 (13°), $(NH_4)_2C_2O_4 \cdot H_2O$ (27°), $(NH_4)_2C_2O_4 \cdot H_2O_2$ (28°), and $BaC_2O_4 \cdot 0.5H_2O$ (30°) remain to be considered. Evidently, in each of these instances the oxalate is involved in significant bonding interactions, i.e., H bonds. This raises the question, whether the strong prevalence of the planar configuration is related to intermolecular interactions rather than to the intramolecular electron density distribution. In order to empirically clarify this issue, we have undertaken a systematic structural investigation of ionic oxalates that exhibit the lowest possible covalent bonding to the cations, i.e., the anhydrous oxalates of potassium, rubidium and cesium.

Due to the hygroscopic nature of the oxalates, only few instances of successful single crystal syntheses of solvent-free oxalates in sufficient size and quality for single crystal analysis have been reported so far: by diffusion ($Ag_2C_2O_4$), slow evaporation from an aqueous solution ($Li_2C_2O_4$, $Na_2C_2O_4$, $K_2Be(C_2O_4)_2$) or hydrothermal crystallization (SrC_2O_4).

Therefore we performed high-resolution X-ray powder diffraction experiments on beamline X3B1 of the Brookhaven National Synchrotron Light Source in transmission geometry to determine the crystal structures of $K_2C_2O_4$ (I), α-$Rb_2C_2O_4$ (II-α), β-$Rb_2C_2O_4$ (II-β), and $Cs_2C_2O_4$ (III) at ambient conditions. In order

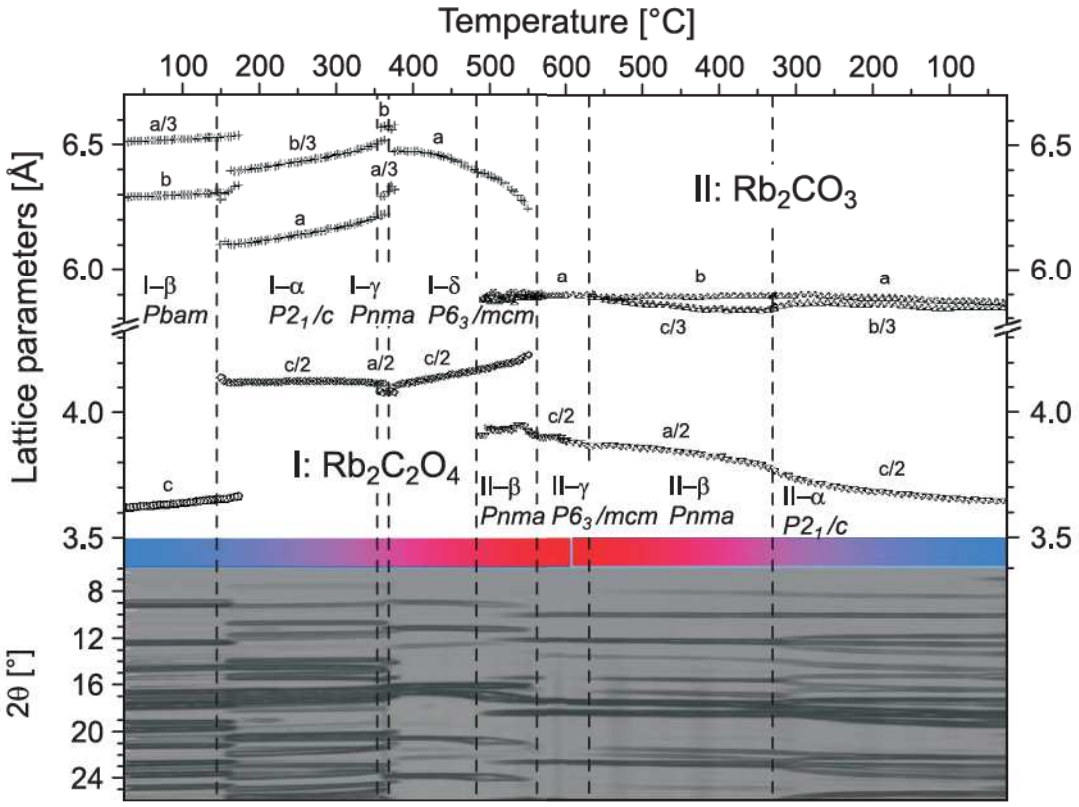

Figure 12: Dependence of lattice parameters on temperature for $Rb_2C_2O_4$ and its decomposition product Rb_2CO_3 during heating up to 600°C (4h) and consecutive cooling down to room temperature (2h) as derived from fast angle dispersive X-ray powder diffraction with an image plate detector (bottom).

to understand order-disorder phenomena and decomposition at elevated temperature, powder samples of $M_2C_2O_4$ (M = K, Rb, Cs) were investigated during heating up to 600°C and consecutive cooling down to room temperature using *fast* angle dispersive X-ray powder diffraction with an image plate detector (beamline X7B, NSLS). By this a variety of new crystal structures of high-temperature phases could be identified and solved. As an example $Rb_2C_2O_4$ (Fig. 12) is given showing four phases of $Rb_2C_2O_4$ and three phases of the decomposition product Rb_2CO_3 (most of which were previously unknown). The crystal structures of the alkali metal oxolates were solved using a global optimization method in direct space followed by consecutive Rietveld refinements using either restraints or rigid body notation.

Freshly prepared anhydrous rubidium oxalate consists of a mixture of two phases with the α-phase (II-α) as the predominating phase. Heating the α-phase above room temperature or storing at room temperature for some time leads to a complete transition into β-rubidium oxalate (II-β). Interestingly, a back-transformation from the β- to the α-phase sometimes occurs upon heating, followed by two additional phase transitions at higher leading temperatures to more or less disordered phases (Fig. 12).

The crystal structures of (I) and (II-β) are isotypic. They can be viewed as distorted AlB_2-type layer structures (3% distortion from hexagonal metric). The center of gravity of the oxalate anion is in the origin of a hexagonal unit cell and two alkali cations are located close

to $\frac{1}{3}\frac{2}{3}\frac{1}{2}$ and $\frac{2}{3}\frac{1}{3}\frac{1}{2}$ (Fig. 13), thus forming alternating layers of oxalate anions and alkali cations. The planar oxalate anions are located on a mirror plane, forming infinite parallel chains along *c*-direction with the length of the *c*-axis as spacer. Each oxygen atom of the oxalate anions is coordinated to four alkali cations. Pairs of potassium cations (distance 3.502(1) Å; rubidium cations 3.643(1) Å) which are interconnected by parallel (C–C bond) oxalates in a zig-zag manner, form infinite parallel double chains along *c*-axis.

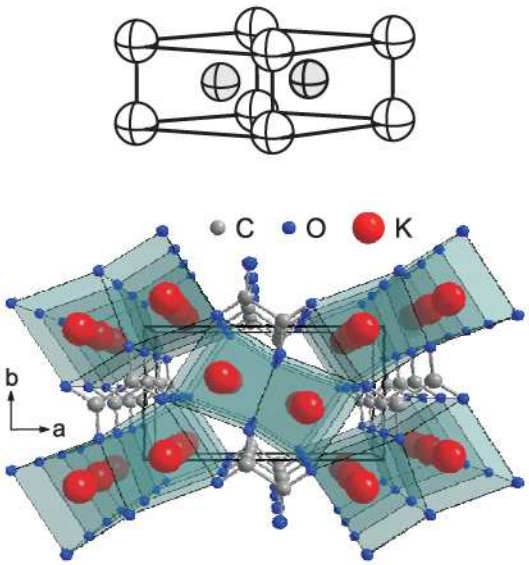

Figure 13: Packing (bottom) and packing scheme (top) of $K_2C_2O_4$ respectively β-$Rb_2C_2O_4$ at ambient conditions.

In *a*-direction, the double chains are alternately inclined by approximately $\pm 20°$ against the *a*-axis, leading to a herringbone arrangement (Fig. 13). Each alkali cation is surrounded by eight oxygen atoms in form of a distorted cube. Two cubes form a pair via a common face, and these pairs are stacked to infinite chains along *c*-axis via common faces. Therefore, each cube shares three faces with neighboring cubes. Four of the side edges of a double cube are shared with four neighboring double cubes. Each oxalate chain is connected to four double chains of alkali cations and vice versa.

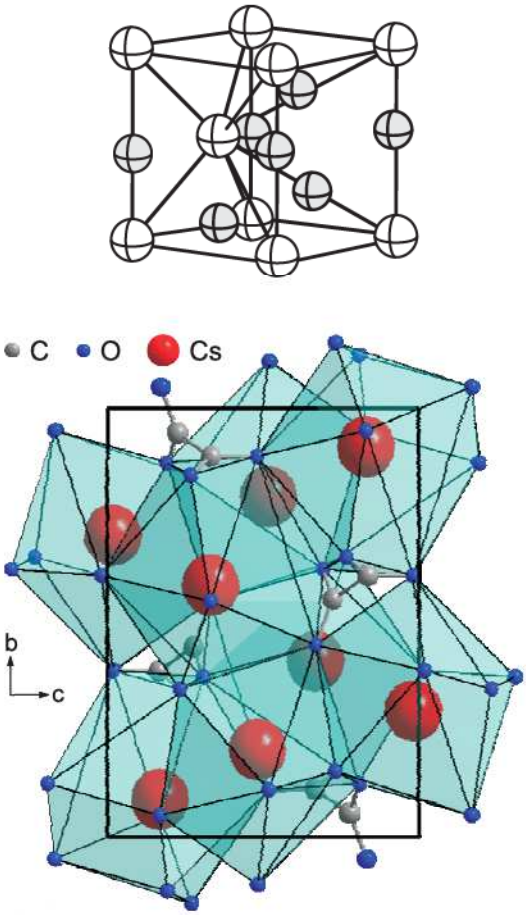

Figure 14: Packing (bottom) and packing scheme (top) of $Cs_2C_2O_4$ respectively α-$Rb_2C_2O_4$ at ambient conditions.

In contrast to the crystal structures of (I) and (II-β), the isotypic crystal structures of (II-α) and (III) are not layer but framework structures (Fig. 14). Each of the two crystallographically different alkali cations is surrounded by a different number of oxygen atoms forming irregular polyhedra. The alkali atoms Cs(1) and Rb(1), respectively, are coordinated to nine oxygen atoms (distances 3.069(9) Å to 3.557(9) Å for cesium; 2.888(6) Å to 3.386(5) Å for rubidium) which belong to six different oxalate anions in form of a distorted tetragonal antiprism capped at one of its trigonal planes. Consequently, two of the oxalate anions are side-on coordinated to the alkali cation, while one is end-on coordinated. Each alkali cation Cs(1)/Rb(1) is sur-

rounded by eight alkali cations (six Cs(2)/Rb(2) and two Cs(1)/Rb(1)) in the second neighbor shell. Two alkali cations are located on top of the tetragonal planes, while each of the remaining six atoms is located on top of a trigonal face. The trigonal faces, built by the two side-on coordinated oxalate anions, are not capped. The alkali cations Cs(2)/Rb(2) are coordinated to ten oxygen atoms (distances 3.015(8) Å to 3.737(9) Å for cesium; 2.816(7) Å to 3.580(7) Å for rubidium) belonging to only five different oxalate anions in form of an irregular polyhedron. This can best be described as a distorted trigonal prism with twisted roof and two additional oxygen atoms capping each of the tetragonal side faces of the prism.

The roof is twisted by approximately 45°. Two end-on coordinated oxalate anions form the tetragonal base plane of the prism. Two oxygen atoms of two different oxalate anions form the roof. One of these oxalates is coordinated with only one oxygen atom therefore having the shortest alkali oxygen distance of 3.015(8) Å for cesium, and 2.816(7) Å for rubidium, respectively, while the other anion is coordinated with three oxygen atoms building one of the two caps. The other cap is formed by a side-on coordinated oxalate anion. Each alkali cation Cs(2)/Rb(2) is surrounded by eight alkali cations (six Cs(1)/Rb(1) and two Cs(2)/Rb(2)) in the second neighbor shell. The position of the centers of gravity of the oxalate anions form a *hcp*-type structure (maximum deviation of 3% and 0.8° from hexagonal metric respectively) with the (idealized) positions of the oxalate anions at $\frac{2}{3}\,\frac{1}{3}\,\frac{1}{4}$ and the alkali cations at 0 0 0, $\frac{1}{3}\,\frac{2}{3}\,\frac{1}{4}$. This is the type of packing found in Ni_2In ($P\frac{6_3}{m}mc$) (Fig. 14).

The oxalate anion itself is twisted by 99(1)° for (III) (94(3)° for (II-α)) (Fig. 11). This can be attributed to packing effects in the cesium (rubidium) compound. The influence of hydrogen bonding as found for other, slightly twisted oxalates can be excluded. The lengthening of the C–C bond of the oxalate anion (> 1.54 pm) is consistent for all oxalates and can be explained by molecular orbital theory.

The crystallographic relationship between these two different crystal structures (*Pbam* and $P2_1/c$) can be understood from the following group-subgroup relationship: $Pbam \rightarrow Pbam$ (doubled *c*-axis, which is not observed) $\rightarrow P2_1/c$. Figures 13 and 14 show the relations of the packing of the two different crystal structures. It is clearly visible that (apart from an internal twist within the oxalate anion) displacive movements of both the alkali cations and the center of gravity locations of the oxalate anions occur. No major rearrangements within the crystal structures are necessary.

It may be speculated that the driving force for the structural phase transition between (II-β) and (II-α) is related to the increased polarizability and/or size of the rubidium cation

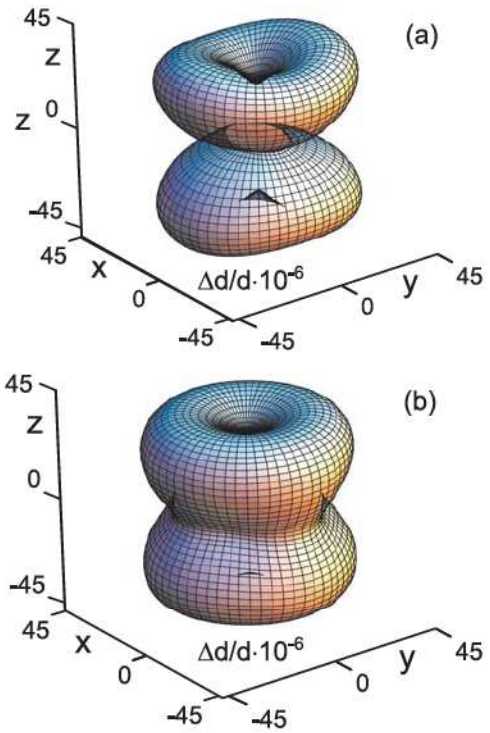

Figure 15: 3-dimensional semi-transparent representation of the microstrain distribution of (a) $K_2C_2O_4$, and (b) β-$Rb_2C_2O_4$ at ambient conditions. The *x*-axis is horizontal, *z*-axis vertical and the *y*-axis points out of the paper. The scale is in $\Delta d/d \cdot 10^{-6}$ strain.

compared to the potassium cation. An unfavorable cation to anion size ratio for a given packing creates stress in certain directions in a crystal structure. This is directly related, via the elastic constants, to the anisotropic microstrain (Fig. 15).

The latter can be derived from high-resolution powder diffraction data. Three-dimensional anisotropic strain distributions of (I) and (II-β) on an equal scale immediately reveal an increase in strain within the layers of alkali respectively oxalate layers with an increase in the size of the cation. In both cases, the strain perpendicular to the layers is relatively low, leaving the packing in the perpendicular direction essentially unchanged. It should be noted that for cesium oxalate, no significant anisotropy of the microstrain was found.

The neutral, solvent-free alkali oxalates clearly show a strong dependence of the coordination numbers on the size of the alkali cations, starting with four (tetrahedron, lithium), six (octahedron, sodium), eight (cubic, potassium and β-rubidium) to nine respectively ten (cesium and α-rubidium).

The structures of the water containing alkali oxalates are completely different from their corresponding anhydrous compounds. As a result, it has become obvious that the conformation of the oxalate anion, when acting as a weak interacting ligand, is mainly determined by packing effects: bonded to non-polarizing cations K^+, Rb^+, and Cs^+, the planar as well as the much rarer staggered conformations have been observed.

Flux-growth and characterization of $NaCu_2O_2$ single crystals

A. Maljuk, A.B. Kulakov, M. Sofin, L. Capogna, J. Strempfer, R.K. Kremer, C.T. Lin, M. Jansen, and B. Keimer

Low-dimensional spin systems are expected to show a rich phase diagram and novel magnetic properties originating from quantum fluctuations. An interesting example is provided by quasi 1D chains of spin ($s = 1/2$) Cu^{+2} ions with competing nearest and next-nearest interactions. From this point the $NaCu_2O_2$ compound should have very interesting magnetic properties. $NaCu_2O_2$ (NCO) was synthesized for the first time over 10 years ago by partial melting of the Cu_2O and Na_2O_2 mixture. The very fine NCO single crystalline grains were mechanically extracted from the inhomogeneous product of reaction [Tams *et al.*, Journal of Alloys and Compounds **189**, 241 (1992)]. Till now no attempts have been made to grow single crystals of $NaCu_2O_2$ compound, probably due to experimental difficulties when dealing with high-reactivity compounds sensitive to moisture and (sometimes) oxygen, showing high volatility of the respective alkaline component and reactivity to all container materials at high temperatures. Here we report the first successful growth of NCO single crystals by the self-flux technique.

DTA-TG analysis was carried out using a NETZSCH STA-449C system. Small amounts of NCO substances were heated in an Ar/O_2 gas flow with the oxygen content of 10^{-3}, 0.2, 5 and 50% respectively. A high-temperature optical microscope (HTOM) 'Olympus' MS-11 equipped with an optical heating system (MS-E1S, 'ULVAC-RICO', Japan) was employed to visualize the melting point of the samples at different oxygen pressures. A compo-